3.23 SHELF DENSE WATER TRANSPORT IN THE BEAUFORT SEA

Meibing Jin* and Jia Wang
University of Alaska Fairbanks, Alaska 99775-7220

ABSTRACT

CTD data from the Beaufort Sea showed fresh surface water of 27 psu in August compared to 31 psu in April, which indicates a saline injection during the winter freezing season. Where and how those cold and salty dense water moves is very important to the halocline formation process.

A coupled ice-ocean model is used to simulate the circulation and ice dynamics and thermodynamics in the Beaufort Sea. With 3.4km horizontal resolution and 16 vertical layers, this nested model obtains open boundary conditions from a similar model with large domain including Arctic and North Atlantic Oceans with 27.5km horizontal resolution. Numerical tracer studies revealed that the rate of dense shelf water penetrating the slope halocline in the Beaufort Sea is low which agrees with results from observations. Sensitivity studies with idealized model identified that salinity stratification is the main reason for the low rate. Wind is important for the position and shape of the horizontal front over the shelf break. Wind and geostrophic flow generated by horizontal salinity front over the shelf break are the two sources of shelf break transports, and among which, wind is the dominant factor. Eddy activities over shelf break generated by salinity front are evident while the shelf break flow along the same direction as the geostrophic flow generated by the front, but in case of reversal of this flow by wind, the eddy activities are also depressed.

1. INTRODUCTION

Dense shelf water plays an important role in maintaining the Arctic cold halocline (Aagaard et al., 1981; Melling and Lewis, 1982; Jones and Anderson, 1986; Martin and Cavalieri, 1989; Cavalieri and Martin, 1994) and also contributes to the formation of deep water in the Arctic (Aagaard et al., 1985; Ostlund et al., 1987; Jones et al., 1995). During the winter season, dense shelf water is formed in the continental Beaufort Sea and eastern Chukchi Sea by brine rejection accompanied by a large amount of ice production in the coastal open water and polynya where the density of the underlying water increased rapidly. CTD moorings in the Barrow Canyon in 1991-1992 showed that salinity reached minimum in fall and maximum in summer for all the stations (Weingartner et al., 1998). The coincidence of salinity maximum with freezing water temperatures manifested that these dense waters formed from the addition of brine during ice formation. The frequency distribution of T/S properties of those CTD moorings showed three modes: the dominant mode had moderate salinities (~32.5) and low temperature (<-1.4°C) characteristic of Chukchi Sea winter water; the second mode had warmer than freezing temperature and intermediate high salinity (33.0~33.6) which came from events of up canyon flow of Arctic Intermediate Water (AIW); the third mode had freezing temperature and hypersaline (>34.0) which was apparently formed over the shelf. If none of these modes mix as they migrate off the shelf, then they are dense enough to ventilate the entire offshore water column between the upper halocline, while the density of the saltiest portion of the hypersaline mode exceeds that of the Canada Basin deep water. These freezing hypersaline water has been reported in the eastern Beaufort sea shelf region too. Melling (1993) found that during some winter, the water overlying Mackenzie shelf in the southeastern Beaufort Sea becomes quit saline (33-35) and at freezing temperature throughout. But those three modes of T/S properties are not separated events. The formation of sea ice is necessary, but not a sufficient condition. Using the observations from the winter of 1980-1981, Melling (1993) illustrated that a two-stage preconditioning of shelf waters is required: first, surface waters of low salinity must be driven off the shelf by strong westerly winds; then, more saline water must rise onto the shelf in response to prolonged easterly winds. So, the third mode (hypersaline freezing water) is formed under the combining efforts of the other two modes: upwelling events provides saline Arctic Intermediate Water to the surface, and then the water is cooled down to freezing and rejected more saline from surface ice formation, finally the increase salinity surpassed that of the halocline of the arctic basin, and ventilation of halocline occurs. Thus, the contribution of dense shelf water to halocline only happens under certain conditions and the chance is low in the Beaufort Sea. Actually, by using observed carbon 14 data, Ostlund et al (1987) indicated a renewal time of the Arctic Bottom Water for about 700 years in the Canadian Basin, and a renewal rate of 30 years for the upper 1500m.

Once the hypersaline water formed, how it is transported offshore and down the slope is also very important on how much the water can contribute to the halocline. As observations are costly and not always available especially in winter, numerical modeling plays an important role to investigate the process of the dense water transport. Some three-dimensional numerical models have been employed to examine the transport of dense shelf water with idealized coastal polynya and uniformly sloping bottom topography. They suggest that both eddy-induced transport and a dense plume near the bottom of shelf break contribute to the offshore transport of the dense shelf water (Chapman and Gawarkiewicz,

* *Corresponding author address*: Meibing Jin, Univ. of Alaska Fairbanks, AK 99775-7220; email: ffjm@uaf.edu.

1995; Gawarkiewicz and Chapman, 1995; Jiang and Garwood, 1996). A salinity front will be developed in the boundary over the shelf break, separating the dense shelf water from the offshore water. The shelf break topography plays an important role in determining a neutral point of stability of the shelf break current and preventing dense shelf water from being transported farther offshore by eddy flux (Kikuchi et al., 1999).

These previous studies provided conceptual and qualitative insight into the dense water transport. However, how well these models can present the situation of Beaufort Sea need to be answered, because dense shelf water sinks as a plume near the bottom of shelf break should be rare, given the slow renewal rate of the Arctic Bottom Water in Canada Basin. In the present study we focus on three-dimensional modeling with realistic ocean stratification of Beaufort Sea. First, we look at some observed temperature and salinity profiles to see any indications of halocline ventilation; second, we performed a numerical passive tracer study based on a three-dimensional coupled ice-ocean model of Beaufort Sea; third, we conducted some sensitivity studies with observed temperature and salinity profile.

2. OBSERVATIONS OF TEMPERATURE AND SALINITY PROFILES

The topography of our interested area is shown in Figure 1. The steep shelf break slope is almost parallel to the Alaska coastline.

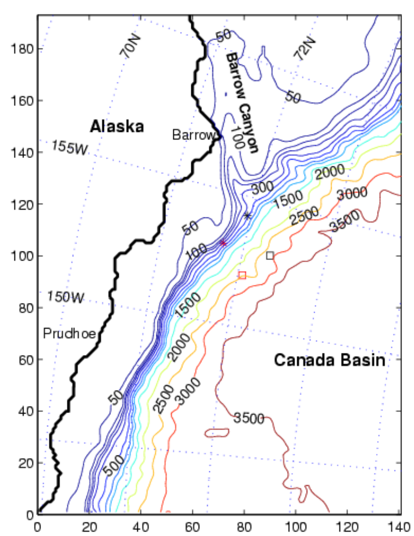

Figure 1: Topography of Beaufort Sea. The black star and square denote station 16 and 21 observed in April 1999; the red star and square denote station 66 and 69 observed in August 1993.

The data of the SCICEX99 (Science Ice Expedition) on the USS Hawkbill submarine unclassified June 1999. These data provided rare CTD profiles in ice-covered Beaufort Sea. Here, two stations (position shown in Fig. 1) observed in April of 1999 are selected to represent temperature and salinity profiles on shelf and shelf break in winter (Figure 2). Another two stations (position shown in Fig. 1) observed in August 1993 are used to represent temperature and salinity profiles on shelf and shelf break in summer (Figure 3).

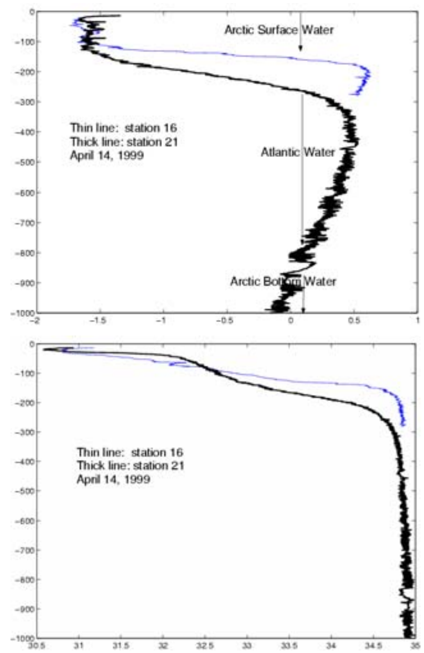

Figure 2: Temperature and salinity profiles of stations 16 and 21.

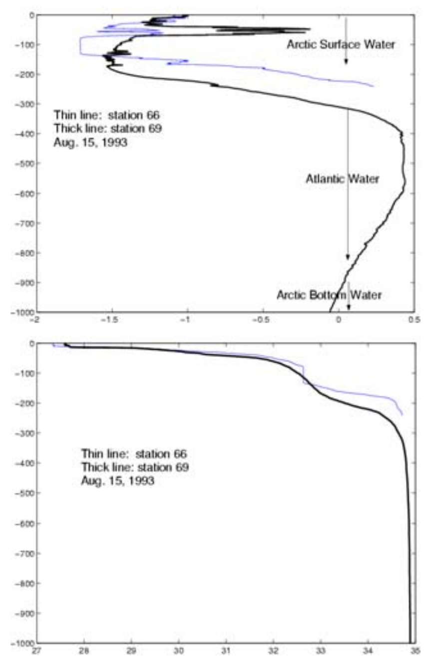

Figure 3: Temperature and salinity profiles of stations 66 and 69.

The typical hydrology and water masses of the Beaufort Sea can be easily identified from the figures 2 and 3: the cold, fresh Arctic Surface Water and warm salty Atlantic Water which occupied the depth range between about 200m and 900m in the Canadian Bain. Its classification as a water mass is justified since it enters the Arctic Ocean from the Atlantic Ocean with distinct properties and can be regarded as formed outside the region. The high salinity provides the Atlantic Water a barrier from mixing with the much fresher Arctic Surface Water. Below the Atlantic Water is the Arctic Bottom Water which has high salinity of 34.9 all the way down to bottom and temperature only changing with pressure.

Seasonal cycle of temperature and salinity can only be seen in the upper 400m because surface cooling in winter alone can't produce water dense enough to penetrate the strong halocline. The surface water is uniformly freezing in winter and slightly warmer in the upper surface layer in summer. The influence of Pacific Water is only seen in summer surface water. The higher temperature and salinity at the bottom of shelf indicates ventilation of halocline in both winter and summer, but for most cases, the ventilation is wind-induced upwelling rather than dense shelf water plume penetrating halocline down the slope.

These CTD profiles suggest the following questions: under upwelling conditions, will the dense shelf water be able to contribute the cold halocline formation? If yes, then what is the pathway of the dense shelf water reaching down to the halocline?

3. NUMERICAL TRACER STUDY

To answer the questions raised above, we conducted a series of numerical tracer studies to examine the percentage rate of the passive tracer released at surface in winter that can penetrate certain depth level. The three-dimensional velocity fields used for the tracer studies were from a coupled ice-ocean model of Beaufort Sea (Wang, Liu and Jin, 2001). The ocean model is POM (Prince Ocean Model, Blumberg and Mellor, 1987). The ice model is a thermodynamic model based on a multi-category ice thickness distribution and a dynamic model based on viscous-plastic sea ice rheology (Hibler 1979, 1980; Thorndike et al., 1975; Yao et al., 2000).

Model domain is shown in figure 1. The model has 16 sigma layers vertically, fine horizontal resolution of 3.4km and is nested in a coarse (27.5km) coupled ice ocean model possessing the same physical process covering the pan-Arctic and North Atlantic oceans. Model forcing includes wind, air temperature, air specific humidity and precipitation interpolated from the monthly mean (except wind is half-daily) of NCEP/NCAR reanalysis data of 1958-1998. Initial temperature and salinity are from PHC 2.0 (Polar Science Center, University of Washington, Steele et al., 2001).

Tracers are released from surface (1m) depth) at six points along shelf edge (Figure 4) in winter months. Because the current field has already contained the density-driven components, the tracer in this study bears no density signature and is passively driven by the three-dimensional current only. At each point, 25 tracers are released one per hour in the first day (December 1) and then calculate till next April 1. Only the averaged trajectories released at same point were drawn in figure 4. Tracers 1, 2, 3 and 6 (were lingering on the shelf and never sinking down to 200m from December 1 to April 1. Also a horizontal front prevented them from moving offshore in the slope current region. The tracers 4 and 5 were the only two getting down below 200m and tracer 4 bounced back and forth around 200m several times while crossing isobaths. As the tracers moved offshore they were also driven west by the slope current and east by currents below halocline.

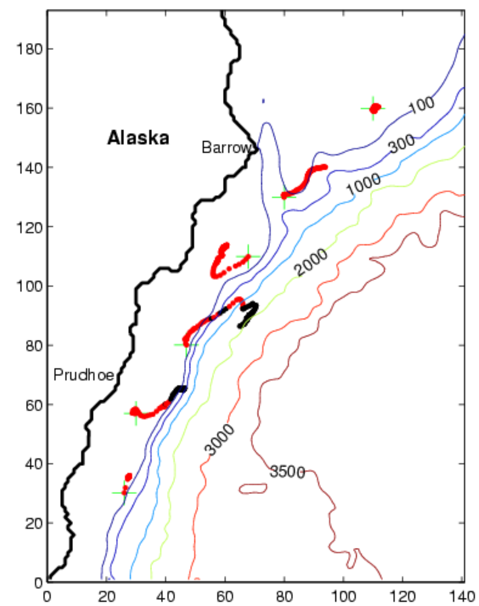

Figure 4: Trajectories averaged from tracers released at six points (marked by '+'): tracer 1 to 6 counting from upright to bottom left. Each dot represents a certain day from December 1 to April 1. Red dots denote the tracers are in the upper 200m, and black denote the tracers are below 200m.

Depth (m)	Tracer No. 1	2	3	4	5	6	Total mean
100	0	64	0	32	68	0	27
150	0	16	0	20	68	0	17
200	0	8	0	20	68	0	16
250	0	8	0	20	52	0	13
300	0	8	0	20	52	0	13
350	0	8	0	20	24	0	8
400	0	4	0	16	24	0	7
450	0	4	0	16	16	0	6
500	0	4	0	16	16	0	6

Table 1: The percentage rates (%)of the tracers penetrating certain depth levels after 120 days

The percentage rates of the tracers penetrating certain levels after 120 days (table 1) showed that rate is going lower with depth especially between the Arctic Surface Water and Atlantic Water ranging from 200m to 350m. The rate also showed large along shelf variances. The total mean of all tracers penetrating halocline is low (under 15%).

When each releasing point was moved 10km toward shore, the averaged trace trajectories (Figure 5) show none of the tracers will sink below 200m or go offshore crossing isobath.

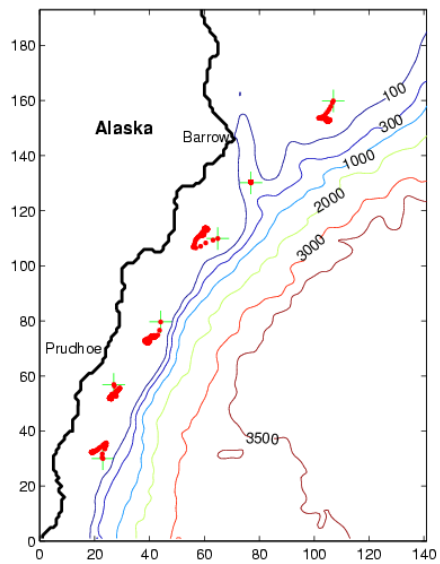

Figure 5: The same as figure but each releasing point of tracer was moved 10km toward shore.

The above results suggest that the dense water produced on the continental shelf far from the edge will not be able to sink to the halocline depth, and even those produced on the shelf edge, the chances penetrating halocline is also very low. This result contrasts sharply with that from idealized model (Kikuchi et al., 1999) in whcih the dense water will sink as a plume along the slope all the way to the bottom of basin, because the idealized model did not have stratification and upwelling-favored wind as the Beaufort Sea.

4. SENSITIVITY STUDY WITH IDEALIZED MODEL

4.1 *Model setting*

To know the importance of stratification and upwelling-favored wind on dense water formation in the Beaufort Sea, sensitivity studies should be conducted by introducing stratification and wind into an idealized model. Here, we use POM (Princeton Ocean Model) with the same model setting, model domain and topography as Kikuchi et al. (1999). Model domain is 300km along shelf and 250km across the shelf. North is from shelf toward offshore (Figure 6). Depth ranges from 30m on the shelf to 600m in the basin. The model has 36 vertical sigma layers and horizontal grid size of 2.5km. the surface salt flux is applied from time t=0 and held fixed for all the calculation time of 180 days. The salt flux of a constant value of -0.5×10^{-4} psu m s^{-1} is used from the coast to y=30km. This value of salt flux corresponds to that of a brine rejection in a coastal polynya where about 700 W m^{-2} of heat flux to the atmosphere is suggested to occur (Martin and Vavalieri,1989; Cavalieri and Martin, 1994). The amount of salt flux decreases with the offshore distance from y=30km and become 1 at y=50km.

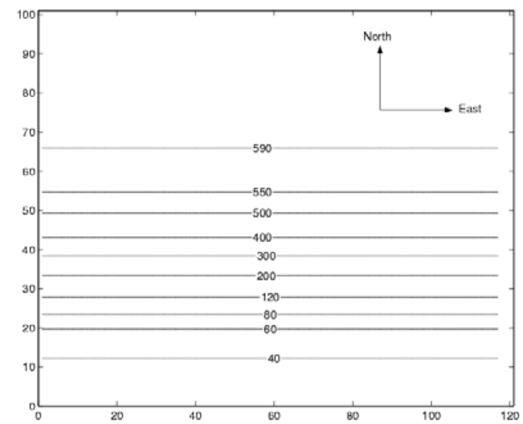

Figure 6: Domain and topography for the idealized model. The axis labels are number of grid points and the grid size is 2.5km.

The following experiment cases are studied: case 1 with stratification but no wind; case 2 with upwelling-favored wind and no stratification; case 3 with stratification and upwelling-favored wind; case 4 with stratification and downwelling-favored wind.

In cases with stratification, the temperature and salinity of station 69 in Figure is set to be the initial condition and the temperature is set homogenous to freezing temperature of –1.5C°. In cases with no stratification, the initial temperature and salinity are set homogenous to 32 psu and –1.5C°.

In cases of upwelling-favored wind, wind is 2.5 m/s from east to west. In cases of downwelling-favored wind, wind is 2.5 m/s from west to east. Here, we choose wind speed 2.5 m/s according to the monthly mean climatologiy wind speed on the shelf break.

4.2 *Results and discussion*

Figure 7 shows a cross-shelf section view of salinity averaged along the shelf for all the four cases. Comparing case 1 and case2 suggests that salinity stratification is the main reason that prevents dense shelf water from sinking all the way down to basin bottom. In no stratification condition, even with upwelling-favored wind, the dense water still went down along the bottom of the slope like a plume, similar to the results of Kikuchi et al. (1999) with no stratification and wind. In cases with stratification (case 3 and 4), upwelling-favored wind makes halocline tilt up toward the shelf and holds more saline on the shelf, while downwelling-favored wind does the opposite. On the surface, a horizontal salinity front was developed over the shelf break region for all cases, separating the dense shelf water from the offshore water. Kikuchi et al. (1999) indicate that the shelf break topography played an important role in determining the position of the front. Here, we can see from Fig. 7 that wind also played an important role in determining the position and shape of the front. In upwelling-favored wind condition, the front is more offshore and straight than that in downwelling-favored wind condition.

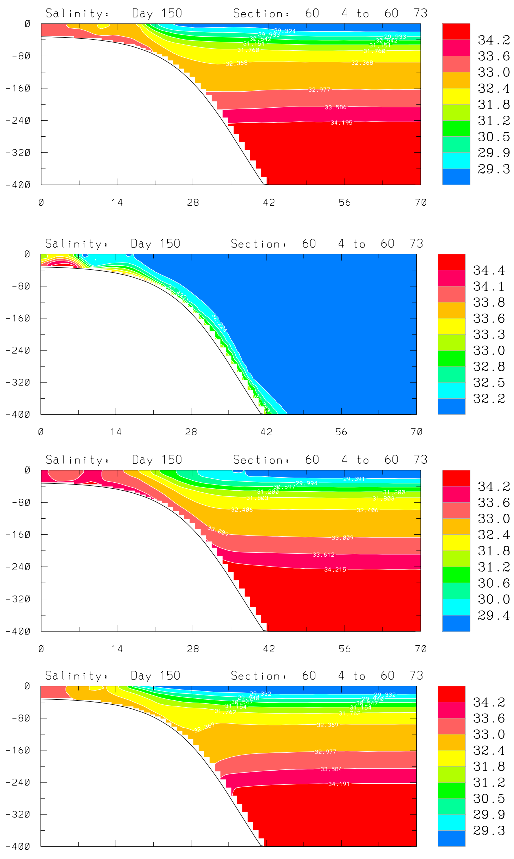

Figure 7: Along shelf averaged salinity section of case 1 at the top to case 4 at the bottom on day 150. The x-axis is from grid 4 to 73.

Wind is found important to the transport along shelf break when comparing the vertically averaged transport of the four cases shown in Figure 8. The shelf break transports are forced by wind and geostrophic current generated by horizontal salinity front over the shelf break. The geostrophic current is toward west. In case 2 of upwelling-favored wind (toward west) and no stratification, the westward shelf break transports are much stronger than that of other cases because the salinity front is much stronger under no stratification condition than others. In cases of stratification, without wind or with upwelling-favored wind (toward west), the shelf break transports are to the west; but with downwelling-favored wind (toward east), the shelf break transports are to the east. Comparing case 1, 3 and 4, we can infer that the salinity front generated transport is about 0.14 Sv, and the wind generated transport is about 1.3Sv, ten times bigger than the former. So, wind is the dominant factor of the shelf break transport.

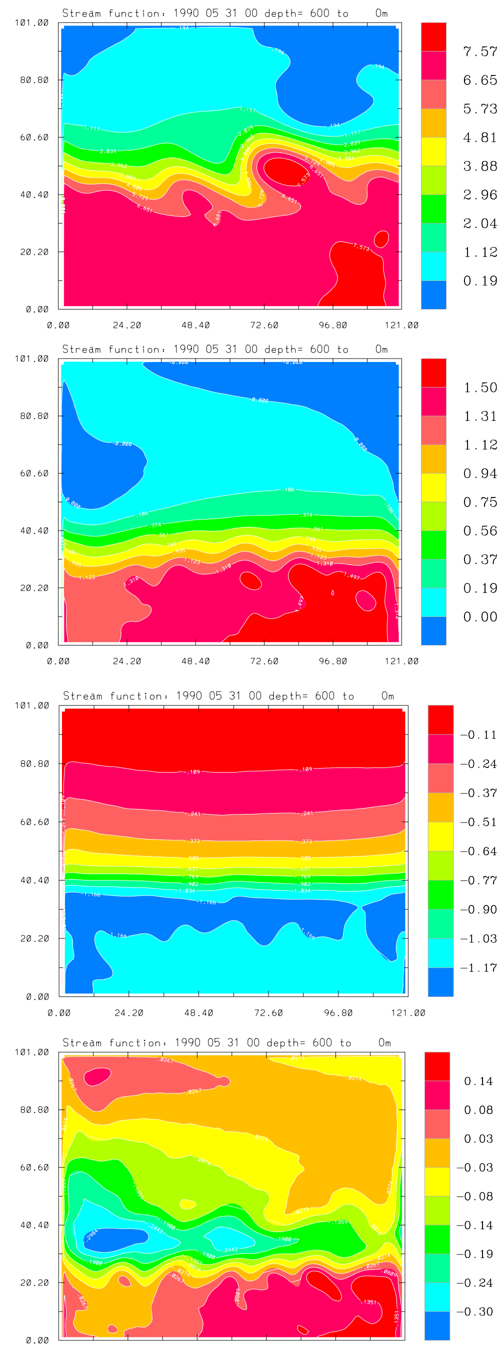

Figure 8: Vertically averaged transport of case 1 at the top to case 4 at the bottom on day 150.

Eddy activities over the shelf break are evident for all the cases with westward shelf break transports but not seen in case 4 with eastward shelf break transports. Because the eddies are generated by the instability of the salinity front over the shelf break, the geostrophic flow generated by the front is westward and the reversal of this flow to eastward by wind in case 4 also depressed the front instability and eddy activities.

5. SUMMARY

Numerical tracer studies using a coupled ice-ocean model revealed that the rate of dense shelf water penetrating the slope halocline in the Beaufort Sea is low which agrees with results from observations and there are two reasons that can explain the low rate: one is strong salinity stratification between the Arctic Surface Water and intermediate Atlantic Water; the other is upwelling-favored wind over the Beaufort Sea.

Sensitivity studies with idealized model identified that salinity stratification is the main reason for the low rate. Wind is important for the position and shape of the horizontal front over the shelf break. Wind and geostrophic flow generated by horizontal salinity front over the shelf break are the two sources of shelf break transports, and among which, wind is the dominant factor. Eddy activities over shelf break generated by salinity front are evident while the shelf break flow along the same direction as the geostrophic flow generated by the front, but in case of reversal of this flow by wind, the eddy activities are also depressed.

Acknowledgements We thank the financial support from the University of Alaska Coastal Marine Institute (Minerals Management Service) and International Arctic Research Center-Frontier Research System for Global Change.

References

Aagaard, K., J.H. Swift, and E.C. Carmack, 1985: Thermohaline circulation in the Arctic Mediterranean Seas. *J. Geophys. Res.*, **90**, 4833-4846.

Aagaard, K., L.K. Coachman, and E.C. Carmack, 1981: On the halocline of the Arctic Ocean. *Deep Sea Res.*, **A28**, 529-545.

Blumberg, A.F. and G.L. Mellor, 1987: A description of a three-dimensional coastal ocean circulation model , *Three-Dimensional Coastal Ocean Model, Coastal Estuarine Sci.*, edited by N.S. Heaps, AGU, Washington D.C. , **4**, 1-16.

Cavalieri, D.J., and S. Martin, 1994: The contributions of Alaskan, Siberian, and Canadian coastal polynyas to the cold halocline layer of the Arctic Ocean. *J. Geophys. Res.*, **99**, 18,343-18,362.

Chapman, D.C., and G. Gawarkiewicz, 1995: Offshore transport of dense shelf water in the presence of a submarine canyon. *J. Geophys. Res.*, **100**, 13,373-13,387.

Gawarkiewicz, G., and D.C. Chapman, 1995: A numerical study of dense water formation and transport on a shallow, sloping continental shelf. *J. Geophys. Res.*, **100**, 4489-4507.

Hibler, W.D., 1979: A dynamic thermodynamic sea ice model. *J. Phys. Oceanogr.*, **9**, 815-846.

Hibler, W.D., 1980: Modeling a variable thickness sea ice cover. *Mon. Weather Rev.*, **108**, 1943-1973.

Jiang, L., and R.W. Garwood Jr., 1996: Three-dimensional simulation of ourflows on continental slopes. *J. Phys. Oceanogr.*, **26**, 1214-1233.

Jones, E.P., and L.G. Anderson, 1986: On the origin of chemical propertities of the Arctic Ocean halocline. *J. Geophys. Res.*, **91**, 10759-10767.

Jones, E.P., P.B. Rudels, and L.G. Anderson, 1995: Deep waters of the Arctic Oceans: Origins and circulation. *Deep Sea Res.*, **I42**, 737-760.

Kikuchi, T. and M. Wakatsuchi, 1999: A numerical investigation of the transport process of dense shelf water from a continental shelf to a slope. *J. Geophys. Res.*, **104**, 1197-1210.

Martin, S. and D.J. Cavalieri, 1989: Contributions of the Siberian shelf polynyas to the Arctic Ocean intermediate and deep water. *J. Geophys. Res.*, **94**, 12,725-12,738.

Melling, H., 1993: The formation of a haline shelf front in wintertime in an ice-covered arctic sea. *Cont. Shelf Res.,* **13**, 1123-1147.

Melling, H., and E.L. Lewis, 1982: Shelf drainage flows in the Beaufort Sea and their effect on the Arctic Ocean pycnocline. *Deep Sea Res.*, **A29**, 967-985.

Ostlund, H.G., G. Possnert and J. Swift, 1987: Ventilation rate of the deep Arctic ocean from canbon 14 data. *J. Geophys. Res.*, **92**, 3769-3771.

Steele, M., R. Morley and W. Ermold, 2001: PHC: A gloval ocean hydrography with a high quality Arctic Ocean. *J. Clim.*, **14**, 2079-2087.

Thorndike, A.S., D.A. Rothrock, G.A. Maykut and R. Colony, 1975: The thickness of distribution of sea ice. *J. Geophys. Res.,* **80**, 4501-4513.

Wang, J., Q. Liu and M. Jin, 2001: A nowcast/forecast model for the Beaufort Sea ice ocean oil spill system (NFM-BSIOS). *Univ. of Alaska Coastal Marine Institute Annual Report* No. **8**, 80-94.

Weingartner, T.J., D.J. Cavalieri, K. Aagaard and Y. Sasaki, 1998: Circulation, dense water formation and outlfow on the northeast Chukchi Sea shelf. *J. Geophys. Res.* **103***:* 7647-7662.

Yao, T., C.L. Tang and I.K. Peterson, 2000: Modeling the seasonal variation of sea ice in the Labrador Sea with a coupled multicategory ice model. J*. Geophys. Res.*, **105**: 1153-1165.